



Title	Abstracts & Titles, No.40-No.42
Citation	Memoirs of the Faculty of Engineering, Hokkaido University, 12(1), 69-97
Issue Date	1967-01
Doc URL	http://hdl.handle.net/2115/37850
Type	bulletin (other)
File Information	12(1)_69-98.pdf



[Instructions for use](#)

Appendix

Abstracts & Titles, No. 40—No. 42

BULLETIN
OF THE
FACULTY OF ENGINEERING
HOKKAIDO UNIVERSITY

NOTICE

Papers and Reports

Author Page

No. 40 (March, 1966)

1. Torsional Buckling of Angle-iron (1st Report) H. Dohba, H. Hanzawa 1
2. An Experimental Study on the Performance of a Multifuel Engine
..... T. Kuroiwa, T. Murayama 13
3. Lateral and Torsional Vibrations of Band Saw Blade (I) T. Kanauchi 35
4. Time Optimal Problem with the Actuator Saturated in its Magnitude
..... M. Kawauchi, S. Koyama, R. Tagawa, R. Miura 67
5. Electron Beam Trajectories in CEF-Type Devices I. Sakuraba 77
6. Imaging Action of Gas Lens Y. Aoki, M. Suzuki 87
7. A Study on Interface Mass Transfer —Effect of Interfacial Tension—
..... M. Kugo, T. Shibata, Y. Kumakawa 95
8. Separation of Straight-Chain Hydrocarbons from Petroleum Fractions by Means
of Urea-Adduct Formation H. Ohtsuka, K. Aomura, T. Musha 125
9. Studies on the Oxo Synthesis
 - I. The Effect of the Synthesis Gas Composition in the Oxonation of Octenes
..... M. Matsubara, M. Ogawa, K. Aomura, H. Ohtsuka 139
10. Studies on the Boron Trifluoride Catalyst
 - Part 2. The Deterioration of the $\text{BF}_3\text{-H}_2\text{O}$ Catalyst in the Alkylation
Reactions at Room Temperature
..... N. Yoneta, K. Aomura, H. Ohtsuka 149
11. Design and Construction of the Nuclear Magnetic Triple Resonance Apparatus
..... S. Shimokawa 163

Torsional Buckling of Angle-iron (1st Report)

Hisanori DOHBA
Hiroshi HANZAWA

Abstract

Hitherto many experimental investigations and some theoretical analyses on column buckling have been performed. However, in most cases studies were made on long columns about λ (slenderness-ratio) ≥ 100 . Furthermore hardly any experimental reports on buckling tests under torsion and compression have been made.

We made some experiments on short angle-iron columns with an apparatus for applying torsional buckling load.

In this paper, the results of torsional buckling for $\lambda=60$ are reported and the following experimental equation is obtained :

$$\begin{aligned}\frac{\sigma_c}{\sigma_y} &\doteq 0.80 - 0.0102 T^2 \\ &\doteq 0.80 - 0.113 \theta^2\end{aligned}$$

where σ_c is the buckling stress, σ_y is the lower yield stress, T is the torque (kg-m) and θ is the angle of twist (rad/m).

An Experimental Study on the Performance of a Multifuel Engine

Tamotsu KUROIWA
Tadashi MURAYAMA

Abstract

The present paper presents the most essentials of the performance and combustion behavior tests of a precombustion chamber diesel engine on a variety of fuels. Two methods of reducing the ignition delay were attempted fairly successfully :

1. Reduction of the heat transfer by promoting the insulating effect of the prechamber with a sleeve to raise its mean wall temperature.
2. Employment of higher compression ratio up to 19.05.

As a result, a possibility of operating a diesel engine on automotive gasoline was assured.

Lateral and Torsional Vibrations of Band Saw Blads (I)

Tadahiko KANAUCHI

Abstract

A band saw blade for lumbering is deformed plastically by stretching.

Furthermore, a pull is created between the two wheels of the band saw machine, and the tensile stress in the cross section amounts to 10~15 kgs per mm².

Under working conditions the running velocity is as high as 40~50 meters per second.

While the blade is very thin, the free parts between both wheels are comparatively wide.

Thus, vibration problems become exceedingly complicated under these conditions.

Now, since the vibrations form uneven or waved surfaces on the lumber face and result in damage to the band saw blade itself, due considerations must be given.

First, it seems necessary to investigate the frequencies of the band saw blade theoretically and experimentally.

In this paper, formulas for the calculation of lateral and torsional frequencies of free parts of the band saw blade were solved under some conditions, and the calculated values using these formulas were shown to give approximately the same results as obtained in the experiments.

Time Optimal Problem with the Actuator Saturated in its Magnitude

Masataka KAWAUCHI, Shoichi KOYAMA, Ryozauro TAGAWA
and Ryoichi MIURA

Abstract

Optimal control signals are often of the Bang-Bang type in such cases where the admissible control variables are limited in their magnitudes. Practical actuators used to an optimal control are subject to some other restrictions. In such a case, the problem must be treated as a problem having a restriction in the phase space, and the analysis becomes considerably difficult.

A method to decide the optimal switching condition for a third-order system

having a restriction was investigated. And success in synthesizing the optimal switching condition was obtained as follows; as a first step, the difference between the characteristics of the idealized second-order system and the practical third-order system was clarified. Then the characteristics of the considering actuator was separated from the system. Thereafter the system was analyzed as a second-order system, and as a final step the switching condition for the second-order system was modified in accordance with the characteristics of the actuator.

Electron Beam Trajectories in CEF-Type Devices

Ichiro SAKURABA

Abstract

This paper deals with the electron flow properties of ribbon-shaped beams in centrifugal electrostatic focusing systems.

The electron motion in radial and linear tangential perturbations is a combination of circular motion with an angular velocity Ω_0 and a simple harmonic motion in a radial direction of angular frequency $\sqrt{2} \Omega_0$. The spatial angle corresponding to one period in radial and linear tangential perturbing influences is the characteristic rippling angle.

The beam in this system carries four space-charge waves: a positive-energy fast wave, a negative-energy slow wave and two synchronous diocotron waves. Propagation constants of fast and slow waves consist of electronic propagation constant, plasma propagation constant and the ratio of angular frequency of simple harmonic motion in the radial direction to angular velocity of circular motion.

The beam stiffness—i. e., the ability of the beam to remain in its equilibrium trajectory under the influence of lateral disturbing forces—is directly proportional to the equilibrium angular velocity of the electron.

Imaging Action of Gas Lens

Yoshinao AOKI

Michio SUZUKI

Abstract

A laminal flow type gas lens using the temperature gradients of air was made and some experiments on the imaging action of the gas lens were made.

The experiments were as follows,

(1) The appearance of real images by light rays through the gas lens were observed while altering the temperature of the surface of the metal pipe.

(2) The appearance of real images, were observed while changing the distance between the gas lens and the imaging plane.

(3) A Keplerian telescope arrangement was made using a gas lens for an object lens and a concave mirror for an eye lens.

As a result of the experiment, the imaging action of the gas lens was ascertained.

A Study on Interface Mass Transfer

— Effect of Interfacial Tension —

Masao KUGO, Toshiharu SHIBATA
and Yoshinori KUMAKAWA

Abstract

A mass transfer through a horizontal interface was investigated by using the acetic acid-benzene-water system which seems to be one of the typical systems having the interfacial turbulence. In this experiment the solute was transferred from the water to the benzene phase.

Among several factors which might be related to the induction of turbulence, a contribution of the interfacial tension upon the turbulence was somewhat illustrated by measurements of the values as follows;

1. Interfacial tensions of this three components system in which the concentration of acetic acid was varied as being in equilibrium in both phases.

2. The tensions at the time just after contact of both phases of which the one was of pure benzene and these time-dependency.

3. These various tensions of the system in which several amounts of a surface active agent were added.

The contribution of acetic acid as well as the surface active agent upon the tension could be illustrated by a following equation:

$$\tau = 34.7 - 1.96 C_{\text{AcOH}}^{0.426} + 2.02 C_{\text{AcOH}}^{0.394} C_{\text{SAA}}^{0.0658} - 28.6 C_{\text{SAA}}^{0.6327}$$

Basing upon evidences in this system resulted from the experiment, such as no change of distribution coefficient by adding the surface active agent as well as rather weak concentration-dependency of the diffusion coefficient, the transfer rate of acetic acid could be calculated by the following empirical correlation which depends upon the concentration-dependency of interfacial tension:

$$W = \frac{C_{w_0}}{\sqrt{D_w m} + \sqrt{D_B}} \sqrt{\frac{4D_w D_B t}{\pi}} \left\{ 1 + k \left(-\frac{dr}{dC_w} \right)_0^{2.0} \right\}$$

In this equation, it might be regarded that the term of tension derivative with the solute concentration is directly corresponding with the effect of turbulence to promote the transfer.

Separation of Straight-Chain Hydrocarbons from Petroleum Fractions by Means of Urea-Adduct Formation

Hiroshi OHTSUKA, Kazuo AOMURA and Takanori MURAHARA

Abstract

Behavior of normal heptane, normal hexane and a mixture of normal heptane and iso octane in urea adduct formation were observed under various reaction conditions.

The results obtained were successfully applied to the separation of straight chain components from the kerosene fractions.

Studies on Oxo Synthesis

I The effect of the synthesis gas composition in the Oxonation of Octene.

Mutsuya MATSUBARA, Masayuki OGAWA, Kazuo AOMURA and Hiroshi OHTSUKA

Abstract

The Oxonation of Octene was studied. The aim of this work was to observe the influence of $H_2:CO$ ratio in the oxonation gas on the conversion rate of olefins and on the composition of the reaction products.

Octene was prepared from commercial 2-ethylhexanol-1 by catalytic dehydration using pelleted bentonite as the catalyst.

The reaction apparatus was an autoclave of 500 cc capacity with a rocking apparatus.

The experiments were conducted under the following reaction conditions.

Reaction temperature: 160°C, 200°C

Initial pressure of synthesis gas at room temperature: 130 atm gauge

Duration of each run: The reaction mixture was maintained at reaction temperatures of 160°C or 200°C, until the pressure drop of the synthesis gas was no longer observed.

The amount of sample olefin used for each run: 50 g

The amount of the catalyst used for each run: 2 wt% cobalt metal of the sample amount

Synthesis gas composition: $H_2:CO=0.28\sim1.84$ ($H_2+CO=95\%$)

The experimental results were summarized as follows:

1. At the reaction temperature of 160°C, the conversion rate of octene and the composition of the reaction products were practically independent of the $H_2:CO$ ratio (0.29~1.80) synthesis gas. The reaction products consisted of ca. 60% of C_8 -aldehydes and ca. 10% each of alcohols, fatty acids and esters.

2. However, at the reaction temperature of 200°C, the $H_2:CO$ ratio showed appreciable effects. The conversion maximum was observed in the neighborhood of $H_2:CO$ ratio of 0.47.

The total amount of oxygenated compounds in the reaction products showed its maximum value (90.4%) in the neighborhood of $H_2:CO$ ratio of 0.47 and its minimum value (39.8%) in the neighborhood of the $H_2:CO$ ratio of 1.84.

Studies on Boron Trifluoride Catalyst

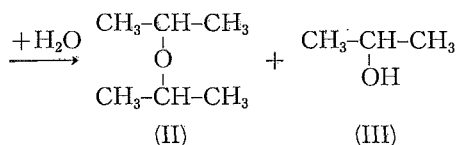
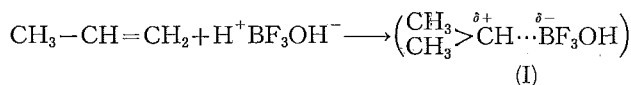
Part 2. The Deterioration of BF_3-H_2O Catalyst in Alkylation Reactions at Room Temperature

Norihiro YONEDA, Kazuo AOMURA and Hiroshi OHTSUKA

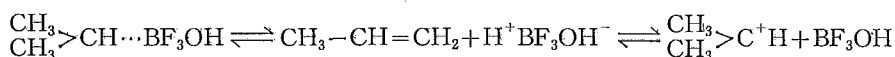
Abstract

The catalytic behaviors of the BF_3-H_2O catalyst in the alkylation of benzene with propylene were observed and discussed with special reference to the deterioration of the catalyst during the course of the reaction at room temperature. The activity of the BF_3-H_2O complex was very high and almost constant for some time in the early stage of the reaction, and then decreased very suddenly. The main cause of the catalyst deterioration was neither the desertion of BF_3 from the catalyst nor the accumulation of propylene polymers on the catalyst but the chemisorption of feed propylene to the catalyst.

By hydrolysis of the spent catalyst, isopropyl ether (II) and isopropyl alcohol (III) were obtained. This result suggested the existence of the ester type intermediate (I) presumably formed by a combination of the chemisorbed propylene with the catalyst.



And the following equilibrium relations might be considered.



The possibility of the spent catalyst regeneration by long standing or heating may be suggested by the above mentioned relations.

Design and Construction of the Nuclear Magnetic Triple Resonance Apparatus

Shigezo SHIMOKAWA

Abstract

The necessary conditions for the double and triple resonance including foreign nucleus such as ^{14}N in the high resolution Nuclear Magnetic Resonance (NMR) spectrometry have been discussed. Based on the discussion the apparatus for the double and triple resonance was designed. The apparatus for the ^{14}N resonance were designed and constructed. The ordinary high resolution NMR spectrometer, which is commercially obtained and bridge type, was modified for the double resonance, that is simultaneous resonance for proton and ^{14}N nucleus. The spin decoupler utilized with the double resonance apparatus for the triple resonance, first resonance for proton resonance for observation, second for resonance for decoupling interaction of proton with ^{14}N and third for proton decoupling. The optimum conditions for power of the second and third r - f field were determined to obtain the most resolved spectra.

This triple resonance apparatus has been applied and successful to obtain the spectra for N-methyl-acetoamide and pyrrole.

NOTICE

Papers and Reports

Author Page

No. 41 (August, 1966)

1. Studies on Copper Converter Slag and Lead Blast-Furnace Slag by the Electron Probe Microanalyser A. Chida, T. Tanaka 1
2. On the Motion of a Wagon Caused by Rapid Starting or Braking T. Irie, G. Yamada 19
3. Study on Surface-finishing with an Elastic Wheel
(I) Scratches on Soft Metals with an Elastic Supported Tool K. Saito, S. Igarashi 37
4. On the High Velocity Deformation of Fe-Si Steel Sheets (I) H. Nakae, K. Tagashira 85
5. Photomixing and Photoelectron-Beam Demodulators for Microwave Amplitude-Modulated Light Signals I. Sakuraba 95
6. Gain Characteristics of CEF-Type Forward-Wave Amplifiers I. Sakuraba, M. Hiraishi 121
7. Photo-electric Properties of Cadmium Sulfide Single Crystal M. Maeda, K. Miyata 135
8. Emitter Dip Effect in Double Diffused Silicon *n-p-n* Transistor M. Maeda, T. Manabe 167
9. A New Technique for Measurement of a Position of Pulsatory Light Beam by Using Some Optical Attenuator K. Sakakibara, K. Kanaya, N. Kodama, S. Fujiki, M. Suzuki 187
10. Studies on Copper Oxide and Adkins' Copper Oxide-Copper Chromate Catalysts H. Ohtsuka, K. Aomura, N. Tomita, K. Hashimoto, O. Takada 199
11. Alkylation of Pentane Fraction with $H_3PO_4-BF_3$ Catalyst H. Sato, K. Aomura, H. Ohtsuka 231
12. Identification of Constituents in C_5 -fractions obtained by Cracking of Petroleum Hydrocarbon M. Itoh, Y. Arai, M. Tokuda 251
13. Studies on Desulfurization of Crude Benzole (I)
Adsorption and Hydrogenolysis of Organic Sulfur Compounds in Crude Benzole over Nickel Catalysts M. Itoh, A. Ishikawa, T. Sato 259
14. Stereoselectivity of Raney Nickel Catalyst on Hydrogenolysis of Bicyclic Monoterpene Epoxides A. Suzuki, M. Miki, M. Itoh 271
15. Studies on Hydroboration (Preliminary Report) A. Arase, M. Itoh, A. Sasaki, A. Suzuki 283
16. Stability of the Functionally Heterogeneous Reactor Y. Ogawa, Y. Ozawa 293
17. Measurement of the Corrosion Rate of Zone-refined Iron in Weakly Acidic and Neutral NaCl Solution by the pH-static Method T. Morozumi 309
18. Studies on Density Current (I)
A Model Study on Salt Wedge M. Kashiwamura, S. Yoshida 327

Studies on Copper Converter Slag and Lead Blast-Furnace Slag by the Electron Probe Microanalyser

Akira CHIDA

Tokiaki TANAKA

Abstract

Recently the electron probe microanalyser has become one of the most powerful tools available for chemical analysis of micro areas of a few microns in diameter on the surface of metals, minerals and other solids.

However, copper converter and lead blast-furnace slags have not yet been investigated by this tool.

The present investigation was undertaken to provide information on the distribution of copper, zinc, lead, cobalt, etc. in these slags. Various compounds crystallized in the slags were also identified by means of microanalysis and X-ray diffraction technique.

The results on the distribution of cobalt between matte and slag were discussed thermodynamically.

On the Motion of a Wagon Caused by Rapid Starting or Braking

Toshihiro IRIE

Gen YAMADA

Abstract

For the purpose of increasing transportation capacity, high speed transportation using large sized aerial ropeway wagons are being introduced recently. However, the present ropeway regulations of this country limit the maximum speed of travelling wagons to 3.6 m/sec, which is far lower than the maximum speed of travelling wagons (9~10 m/sec) of countries in Europe and America. Hence, a revision of regulations is suggested in an attempt to raise the speed level.

As part of basic studies on this problem, the vibration of the wagon and the change of tension of ropes caused by starting or braking were studied owing to its importance in planning and designing a wagon travelling at high speed. In this paper, in an attempt to study the problem theoretically some basic equations of

motion of the wagon were introduced and a block diagram was presented.

It was concluded from the theoretical calculation that the angular displacement of a wagon with a damper of large capacity is small, while no effects of damping are seen in the angular acceleration of the wagon. Under usual starting or braking conditions (less than 0.1 g), the change of tension has little direct effect with respect to strength, but the vibration of aerial rope systems including the wagon caused by such starting or braking requires careful consideration.

Study on Surface-finishing with an Elastic Wheel

I. Scratches on Soft Metals with an Elastic Supported Tool

Katsumasa SAITO
Satoru IGARASHI

Abstract

In order to determine the mechanism of surface-finishing of soft metals with an elastic wheel, it is necessary to clarify the cutting mechanism of one single grain adhered to the surface of the wheel with some elastic material. For this purpose, scratch tests for Al-alloy plates and a Copper plated aluminum plate were conducted with an elastic supported diamond cone tool, which was considered as a model of a single grain on the surface of the elastic wheel.

In this report, the scratches on a finished soft metal surface were observed under microscope and the scratch dimensions were precisely measured by means of a light-cut method. The dynamic characteristics of the elastic materials used and the micro-Vickers hardness of the soft metals were measured. And the structure of the soft metals was examined under microscope.

The results obtained were follows:

- 1) The motion of the tool during scratching was explained from the character of force applied to the tool and the dynamic characteristics of the elastic materials used.
- 2) With the decrease of spring constant the shape of the longitudinal section of the scratch changed gradually from a circle arc to a shape resembling a ship bottom, and the sliding track extended at both ends of the scratch in the direction of the motion.
- 3) The shape of the pile-ups at the edges of the scratch changed according to the mechanical properties and structures of the specimens.

On the high velocity deformation of Fe-Si steel sheets

Hitoshi NAKAE

Kosuke TAGASHIRA

Abstract

High velocity deformation of Fe-Si steel sheets was studied on both single crystal and polycrystal specimens.

Under a deformation velocity of 20 m/sec, no mechanical twins were observed in fine grained specimens; whereas these were always found in both coarse grained and single crystal specimens.

At the grain boundaries, the twins were often branched or decomposed into many short parallel line twins. As the velocity increased, the hardness of specimens decreased. The dislocations formed a cell structure at static deformation, and random clusters at high velocity deformation.

In recrystallization, the nuclei often originated at the cross point of twins.

Photomixing and Photoelectron-Beam Demodulators for Microwave Amplitude-Modulated Light Signals

Ichiro SAKURABA

Abstract

This paper reviews the early experiments on the photoelectric mixing process and reports on the recent trends of photoelectron-beam demodulators in the United States of America and Europe.

Rapid advances in detection techniques are expected. Microwave photoelectron-beam systems and photodiodes are the leading contenders.

Gain Characteristics of CEF-Type Forward-Wave Amplifiers

Ichiro SAKURABA
Masaaki HIRAISHI

Abstract

This paper deals with the gain characteristics of CEF-type forward-wave amplifiers in a special case where $b=0$, $d=0$, $Q=0$, $\beta_e \approx 20$ and $C \approx 0.05$.

The small-signal forward-wave gain was yielded by

$$\text{Gain (db)} = 10 \log_{10} \left[\cosh^2 \frac{\sqrt{\beta_e C}}{2} \phi + \frac{9}{8\beta_e^2} \sin^2 \frac{\sqrt{2}}{\beta_e C} \phi \right].$$

The first term is due to the growing and decreasing waves in the beam-circuit system and the second term is due to the characteristic ripple in the CEF-type focusing system. Under the condition where $\beta_e \approx 20$ and $C \approx 0.05$, the second term is negligible so that the gain can be approximated by

$$\text{Gain (db)} \approx 10 \log_{10} \left[\cosh^2 (\pi CN \sqrt{\beta_e C}) \right].$$

The small-signal gain of CEF-type devices is larger than that of O-type devices for $CN > 0.3$. Because the O-type electron beam has no bunched current and the CEF-type beam has synchronous diocotron effects. For $CN > 0.3$ the gain of O-type devices is much larger than that of CEF-type devices because of the growing slow-space-charge wave. The gain of M-type devices predominates over the other two, because the energy transfer is due to the excess electrons in the retarding region through phase focusing and is due to the motion of these electrons towards the slow-wave circuit.

Photo-electric Properties of Cadmium Sulfide Single Crystal

Masao MAEDA
Kenji MIYATA

Abstract

Photo-electric properties of CdS single crystals (wurtzite type) prepared by sublimation method are reported. Measurements of photoconductivity, rise and decay characteristics of photocurrent and their temperature dependency and conductivity glow curves are used to determine the defect electronic levels in the crystals.

Two types of crystals are clearly distinguished in terms of the defect levels.

The effect of surface treatment, which has been ignored in the case of thin samples, on the surface conductivity and red luminescence are also described. Donor level of about 0.8 eV are supposed to localize in surface region and identification of other electronic levels are remained unaccomplished in this report.

A new model about the electronic transition is proposed in order to explain the experimental results.

Emitter Dip Effect in Double Diffused n - p - n Silicon Transistor

Masao MAEDA

Toyotaka MANABE

Abstract

In the process of manufacturing n - p - n silicon transistors by diffusion technique, very interesting phenomena known as the emitter dip effect are often observed. The origin and the effect on the electrical characteristics of the device are not yet fully understood.

This paper describes the results of a direct observation of diffusion induced dislocations by the etching technique. Diffusion induced dislocations play a decisive role in revealing the emitter dip effect. The main conclusions obtained are as follows; (1) The necessary conditions for the emitter dip effect are the steep concentration gradients of donor impurity at the emitter junction. (2) Dislocation density increases by one or two orders of decades after the impurity diffusion. (3) Dislocation mechanism can not explain the fact that this effect is not observed in p - n - p junctions.

A New Technique for Measurement of a Position of Pulsatory Light Beam by Using Some Optical Attenuator

Katsuaki SAKAKIBARA, Kouji KANAYA, Nobuyuki KODAMA,
Shigeo FUJIKI and Michio SUZUKI

Abstract

A new technique for the precise measurement of a position of pulsatory light beam by using a triangular-type optical attenuator has been found. The principal

arrangement is shown in figure 6, and the apparatus in our experiments is presented in the photograph VI.

The optical attenuator converts the variations of light beam position into intensity variations. These intensity variations can be memorized electrically by memory syncroscope through a multiplier phototube. Consequently the position of pulsatory optical beam can be readily observed.

A triangular cell filled with a solution of cupric sulfate was used in our experiments as a converting attenuator. Our apparatus can accurately detect the displacement of 2/9 mm, and the data is shown in figure 10 and photograph IX.

The necessary pulse width of light in order to detect its position is determined by the sweep time of memory syncro scope, and so generally it is one micro second.

Studies on Copper Oxide and Adkins' Copper Oxide-Copper Chromate Catalysts

Hiroshi OHTSUKA, Kazuo AOMURA, Nobu TOMITA,
Kazuaki HASHIMOTO and Osamu TAKADA

Abstract

As regards copper oxide and Adkins' copper oxide-copper chromate catalysts, the influence of the catalyst composition and the catalyst crystal structure on the catalytic activity was observed mainly by means of X-ray diffraction. The change in the catalyst activity with the change in the catalyst composition during the course of the reaction was also observed. An effective regeneration method for the waste Adkins, catalyst was proposed.

Alkylation of Pentane Fraction with $\text{H}_3\text{PO}_4\text{-BF}_3$ Catalyst

Hideo SATO, Kazuo AOMURA and Hiroshi OHTSUKA

Abstract

When straight run gasoline is used as the feed stock for naphtha cracking or naphtha reforming, its light fraction is usually removed. This light fraction, the so called "pentane fraction", mainly consists of C_5 -and C_6 paraffins. Its iso-paraffin/normal paraffin ratio is about 50:50.

The alkylation of the pentane fraction with propene or isobutene in the presence

of $\text{H}_3\text{PO}_4\text{-BF}_3$ catalyst was studied with special reference to the production of high octane motor fuel.

The olefins were conducted into the four necked-flask with a stirrer containing the pentane fraction and the catalyst under atmospheric pressure.

The products, separated from the unreacted pentane fraction, mainly consisted of isoparaffine with a small amount of olefin polymers.

Both olefins produced the mixtures of C_8 -and C_9 isoparaffins as the alkylates. In the case of isobutene, the main components of the alkylates were methylheptanes. While, in the case of propene, dimethylhexanes were the predominant components of the alkylates.

The maximum conversion of the pentane fraction into the alkylate was about 60%. This figure showed that a small part of normal paraffins presumably participated in the alkylation reaction.

Identification of Constituents in C_5 -fractions obtained by Cracking of Petroleum Hydrocarbon

Mitsuomi ITOH, Yoshio ARAI and Masao TOKUDA

Abstract

Constituents composed of C_5 -fraction (b.p. 20–60°C) obtained by catalytic cracking of petroleum products were identified by the following procedure and instrumental methods. The samples were rectified and fractionated to several narrow cuts by use of a rectifying column which had a high efficiency with more than 80 theoretical plates. Then these narrow fractions were analysed by means of gas-chromatography and the boiling points of each of the detected components could be assumed from the boiling range of the fraction in which the peak height of the component in the chromatogram was maximum. The saturated portion of the fraction could be isolated from other components by means of Kattwinkel reagent treatment. At the same time by using molecular sieves, n-paraffins and n-olefins could be isolated from other hydrocarbons, in each gas-chromatogram of such treated samples the different types of hydrocarbons could be distinguished respectively. For the determination of dienes the Diels-Alder reaction was adopted. By the above described methods and procedures, the main components which were also fractionated by gas chromatography, were also determined by infra-red spectroscopy with standard reference samples.

As a result the identified components were as follows ;

n-Paraffine : n-Pentane and n-Hexane

Isoparaffins : Iso-Pentane, 2-Methylpentane and 3-Methylpentane
 Olefins : Pentene-1, Pentene-2 (trans & cis),
 3-Methylbutene-1, 2-Methylbutene-1,
 2-Methylbutene-2, 2-Methylpentene-1,
 Diolefins were not detected in FCC products but were contained in appreciable amounts in thermal cracking products.

Studies on Desulfurization of Crude Benzole (I)

Adsorption and Hydrogenolysis of Organic Sulfur Compounds in Crude Benzole over Nickel Catalysts

Mitsuomi ITOH, Akio ISHIKAWA
 and Takashige SATO

Abstract

The removal of sulfur, especially organic sulfur compounds, from crude benzole has long been the subject of industrial research in relatively small scale commercial plants, which can not afford the expenses of high pressure hydrodesulfurization.

In this report, as one of the studies on the atmospheric desulfurization, desulfurization by means of adsorption and hydrogenolysis of organic sulfur compounds in commercial benzole over nickel catalysts is described.

In order to produce an extra pure benzene from commercial benzole, it is necessary that the organic sulfur content in the products should be lower than 1.0 ppm. As a first step in the studies, a complete desulfurization was attempted and a search for optimum conditions for atmospheric desulfurization of benzole over nickel catalyst was instituted.

As the second step, the desulfurization ability of nickel to some sulfur compounds (thiophene, carbon disulfide and ethylmercaptane) was studied kinetically.

From the experimental results, it was found that the desulfurization by nickel catalysts was very effective under the following conditions,

Reaction temperature: 100–200°C

Liquidphase space velocity of benzole: 1–5

Gaseous space velocity of hydrogen (or Mixed gas with nitrogen); 10

Sulfur contents of sample: 20–300 ppm (as thiophene)

Kinetic orders of reaction in this process were 0.76th and 1.02th for thiophene and ethylmercaptan respectively, and sulfuration activities of each reagents for nickel changed in the order of $C_2H_5SH > CS_2 > C_4H_4S$ and it seemed that the decomposition of thiophene over the catalyst was the rate determining step.

Stereoselectivity of Raney Nickel Catalyst on Hydrogenolysis of Bicyclic Monoterpene Epoxides

Akira SUZUKI, Mutsuo MIKI
and Mitsuomi ITOH

Abstract

Stereoselectivity of Raney nickel catalyst on hydrogenolysis of bicyclic monoterpene epoxide, α -pinene oxide, 2,3-epoxy bornane, α - and β -epoxy caranes is reported here.

The hydrogenolyses of the epoxides were carried out in ethanol under high hydrogen pressure (95–100 atm.) and at 90–100°C, using Raney nickel only and with a small amount of sodium hydroxide. The obtained products were analyzed by vapor phase chromatography (Golay Carbowax 20 M column-50 m) and were identified by comparison with authentic samples.

The results are summarized in Table 1, 2, 3, and 4.

From these results, it may be considered that the epoxides were hydrogenated predominantly in S_N1 type reaction, in which the oxygen atom of epoxide ring was located upon the surface of catalyst. Hydrogenolysis with inversion was increased by addition of sodium hydroxide except in the case of α -pinene oxide, because of the weak affinity of the catalyst system for oxygen atoms. The steric hindrance of gem-dimethyl group seems to be one of the reasons why the additive effect of sodium hydroxide is not remarkable in α -pinene oxide. Moreover, the structures of these bicyclic monoterpene epoxides, α -pinene oxide, 2,3-epoxy bornane, α - and β -3,4-epoxy caranes were confirmed to be V, XII, XIX and XXI, respectively.

Studies on Hydroboration

(Preliminary Report)

Akira ARASE, Mitsuomi ITOH, Akira SASAKI
and Akira SUZUKI

Abstract

As a preliminary examination of the studies on synthesis of α -olefin from its internal isomers by means of hydroboration technique, the preparation of starting

materials such as pentene, diborane and 1-pentylborane, and the analysis of alkylboranes were studied.

(1) Pentene was prepared by dehydration of pentanol-1 in the presence of bentonite and molecularsieve-13 X as catalyst. The pentene mixture thus obtained was analyzed by vapor phase chromatography. Although bentonite gave lower yields of pentene and lower contents of 2-pentene than molecularsieve-13 X, the former was superior in a point of inertness to isomerize the carbon skeletons.

(2) The vapor phase chromatographic analysis of alcohols which should be obtained in the alkaline hydrogenperoxide oxidation of alkylboranes was examined in detail. Sufficient accuracies were obtained for propanol-1, propanol-2, pentanol-1 and pentanol-2, and it was also found that the method was effective for the analysis of alkylboranes.

(3) A mixture of pentenes (1-pentene 26.2%, 2-pentene 73.8%) was quantitatively hydroborated to pentylboranes with diborane in THF. Finally, it was demonstrated that 95.2 per cent of the borane is found in the 1-position with 4.8 per cent in the 2-position by heating the pentylborane mixture at 185°C.

Stability of the Functionally Heterogeneous Reactor

Yuichi OGAWA

Yasutomo OZAWA

Abstract

A practical and concrete method for analysing the reactor stability is derived. The discrimination of the stability, the region of its existence and also the start-up characteristics are determined by considering the effect of the functional heterogeneity of the reactor system. For this purpose, non-linear integral kinetic equations containing the effects of the delayed neutrons, and of two internal feedbacks of quick and slow responses toward the reactivity are set up and analysed by considering the effects of heat exchange between the heterogeneous structural elements and of the coolant speed which were ignored in V. N. Andreiev's treatment.

The integral equations are transformed into four non-linear simultaneous ordinary differential equations of the first order from which two important singular points are produced, one corresponds to zero out-put and the other corresponds to a certain definite out-put. Assuming the linear approximation in the vicinity of these singular points, one obtains the quadratic algebraic equations at both points. These equations allow us to discuss the stability of the reactor both at the starting point and the operating out-put point.

These algebraic equations can be simplified in great deal under the condition of $C_m \gg C_f \gg C_c$, where C_m , C_f and C_c are the heat capacities of the moderator, fuel and the coolant of the reactor respectively. Applying the condition of the Hurwitz's polynomial to the simplified algebraic equation we can obtain four crossing hyperbolas and one cubic curve which determine the stable region of the reactor at the singular point which corresponds to the definite out-put.

This theory was applied to a Calder Hall type reactor as an example. The results of the numerical calculation are presented in the form of diagrams.

The treatment may be useful for the rapid evaluation of the stability of the heterogeneous reactor at any operating condition.

Measurement of the Corrosion Rate of Zone-refined Iron in Weakly Acidic and Neutral NaCl Solution by the pH-static Method

Takashi MOROZUMI

Abstract

The corrosion rate, the corrosion potential and the polarization curves were determined in the H_2 -saturated NaCl solution under a condition of constant pH maintained with the electrochemical pH-stat. As the previous investigators pointed out, the corrosion rate varies in proportion to the -0.5 th power of pH and the corrosion potential moves toward a more basic potential by the amount of $2.303 RT/F$ per each decade of pH in the pH region less than 4. However, the change of corrosion rate at higher pH is rather complex; namely the rate changes in inversely proportional wise to pH at pH 5, becomes nearly independent of pH at pH 6 and decreases rapidly at pH higher than 7.

These variations of corrosion behavior according to pH were explained by postulating several different reaction steps which control the reaction rate of the local anode and the local cathode of the corrosion cell.

The degree of hydrolysis of the dissolved ferrous ion was also determined under the same experimental conditions as in the corrosion studies. It is found that the formation of $FeOH^+$ complex-ion is remarkable in alkaline solution but insignificant both in neutral and in weakly acidic solutions. A new method for determining the hydrolysis constant of metallic ion was devised by utilizing the electrochemical pH-stat.

Studies on Density Current I

— A Model Study on Salt Wedge —

Masakazu KASHIWAMURA

Shizuo YOSHIDA

Abstract

This paper is the first among a systematic series of studies on density current.

Dynamical properties of a density current in a gravitational field are important particularly in a geophysical sense and is a matter of great interest. In the present paper, the authors dealt with a model study on a salt wedge with an outflow of fresh water.

A dimensionless relationship between the length of the salt wedge and a discharge of fresh water, and a longitudinal figure of the salt wedge were examined in the experiment and tested by a theory. Furthermore, stream lines of the outflow of fresh water were observed and a transition of the stream lines from an exponential figure into a parabolic jet stream are briefly discussed.

NOTICE

Papers and Reports

Author

Page

No. 42 (January, 1967)

1. Two-dimensional Wake in a Simple Shear Flow M. Kiya, M. Arie 1
2. Study on Surface-finishing with an Elastic Wheel (II)
The Optimum Condition of Mirror-finishing of
Grass with a PVA Wheel T. Yuta, K. Saito, T. Nakamura 11
3. The Effect of Electron Injection Velocity Variations on Gain Characteristics of
CEF-Type Forward-Wave Amplifiers I. Sakuraba, M. Senda 29
4. A New Type of Compensation Device for Loss due to Curved Circular TE_{01}
Mode Waveguide " TE_{01} Mode Regenerating Converter" (I)
..... M. Imai, T. Matsumoto 43
5. Effect of Viscosity on Longitudinal Mixing in Gas Bubble Column
..... G. Takeya, T. Ishii, Y. Murai 71
6. Bubbles and Mixing in Gas Bubble Column under Pressure
..... G. Takeya, T. Ishii, K. Makino,
..... M. Makabe, Y. Shiroto, T. Sato 81
7. Time Optimum Control for a Reactor with Two Types of Internal Feedback
..... Y. Ogawa 91
8. Measurement of the Corrosion Rate of Aluminium in NaCl Solution by the
pH-static Method T. Morozumi 123
9. An Electrochemical pCl-stat and Its Application to Electrometric Determination
of Chloride Ion H. Ohashi, T. Morozumi 133

Two-dimensional Wake in a Simple Shear Flow

Masaru KIYA
Mikio ARIE

Abstract

The velocity distribution in the wake of a two-dimensional body located in a simple shear flow is described. With the assumption of constant eddy viscosity the components of velocity are expanded into the power series of small $\omega d/U_0$, where ω is the transverse velocity gradient of the oncoming stream, d is the representative length of the body and U_0 is the velocity of the approaching flow at the centre of the body. The spread of the wake is found to be greater towards the side of the smaller velocity than on the side of the larger one as would physically be expected. It is also shown that the effect of the transverse velocity gradient of the oncoming flow on the drag coefficient of the body is of a higher order than the first power of $\omega d/U_0$.

Study on Surface-finishing with an Elastic Wheel (II)

The Optimum Condition of Mirror-finishing of
Glass with a PVA Wheel.

Toshio YUTA
Katsumasa SAITO
Tsuneo NAKAMURA

Abstract

The PVA wheel has excellent polishing characteristics for the mirror-finish of glass. This wheel consists of agglomerated abrasives using foamed polyvinyl acetal resin as the bond material.

As well known, the polishing characteristics of the PVA wheel is greatly influenced by its composition. However, inasmuch as the PVA resin used as the bond material is sensitive to the environment, it is somewhat hygroscopic.

A series of experiments was carried out to find a key to the optimal performance of the PVA wheel under various conditions.

The results were as follows:

(1) The polishing characteristics of the PVA wheel were found to be very sensitive to the atmospheric humidity. Hence, the composition of the wheel mate-

rial was changed according to the humidity to obtain good polishing characteristics.

(2) The average mechanical properties of the PVA wheel having excellent polishing characteristics were as follows regardless of their composition.

γ_1 (instantaneous rigidity)=1.8 kg/mm², γ_2 (retarded rigidity)=7.5 kg/mm² and η (viscosity)= 1.9×10^{12} poise.

(3) The PVA wheel worked satisfactorily, only when its surface was somewhat hardened by rubbing. The hardened surface had an apparent spring constant of around 0.5 kg/mm measured by a spherical indenter.

The Effect of Electron Injection Velocity Variations on Gain Characteristics of CEF-Type Forward-Wave Amplifiers

Ichiro SAKURABA
Masahiko SENDA

Abstract

This paper deals with the effect of electron injection velocity variations on the gain characteristics of CEF-type forward-wave amplifiers in a special case where $d=0$, $Q=0$, $\beta_e \approx 20$ and $C \approx 0.05$.

The small-signal forward-wave gain for small values of b was yielded by

$$\begin{aligned} \text{Gain (db)} \approx 10 \log_{10} & \left[\cosh^2 \frac{\sqrt{\beta_e C}}{2} \sqrt{1 - \frac{3}{4\beta_e C} \left(b + \frac{3}{\beta_e^2 C}\right)^2} \phi \right. \\ & \left. + \frac{9}{8\beta_e^2} \sin^2 \frac{\sqrt{2}}{\beta_e C} \sqrt{1 + \frac{3}{32} \beta_e^2 C^2 \left(b + \frac{3}{\beta_e^2 C}\right)^2} \phi \right] \end{aligned}$$

The first term is due to the growing and decreasing waves in the beam-circuit system and the second term is due to the characteristic ripple in the CEF-type focusing system. Under the condition where $\beta_e \approx 20$ and $C \approx 0.05$, the second term is negligible hence the gain can be approximated by

$$\text{Gain (db)} \approx 10 \log_{10} \left[\cosh^2 \left(\pi C N \sqrt{1 - \frac{3}{4\beta_e C} \left(b + \frac{3}{\beta_e^2 C}\right)^2} \right) \right]$$

An important feature is the narrowing of the curves with the increasing interaction length, which means the beam voltage is more critical for larger angle devices.

**A New Type of Compensation Device for Loss due
to Curved Circular TE_{01} Mode Waveguide
“ TE_{01} Mode Regenerating Converter” (I)**

Masaaki IMAI
Tadashi MATSUMOTO

Abstract

In this paper, a new method to compensate for mode conversion loss due to bending of circular TE_{01} mode waveguide used in the transmission of millimeter wave is presented.

The method is as follows:

(1) First, the incident TE_{01} mode and the unwanted TM_{11} mode with a phase difference of $\pi/2$ between each other were converted to the rectangular TE_{10} mode through a series of coupling holes.

(2) Secondly, the rectangular TE_{10} mode was converted to the primary circular TE_{01} mode by the same means.

As a result, it is the expectation that the influence of the bend will be removed regardless of the radius of the bend.

The principle there of was investigated theoretically, and examples of actual design, and performance characteristics were presented for 34, 50 Gc as the center frequency.

Farthermore, various problems anticipated to be important in practice were considered in detail.

**Effect of Viscosity on Longitudinal Mixing
in Gas Bubble Column**

Gen TAKEYA
Tadao ISHII
Yasuo MURAI

Abstract

The effects of viscosity of liquid on the longitudinal mixing in a gas bubble column ($Z=125$ cm) with a single orifice have been studied. A gloiopeltis glue solution and nitrogen gas were used. The scope of the experiments was $\theta=39\sim99$

min., $G=0\sim 20$ cm³/min., $\mu=1\sim 41.5$ c.p. The longitudinal dispersion coefficients, E , calculated from the residence time curves were affected greatly by gas velocity and slightly by liquid viscosity, but hardly by θ .

Bubbles and Mixing in Gas Bubble Column under Pressure

Gen TAKEYA, Tadao ISHII, Kazuo MAKINO,
Masataka MAKABE, Yoshimi SHIROTO
and Takashi SATO

Abstract

The behavior of bubbles and the longitudinal mixing characteristics in a gas bubble column with a single orifice have been investigated under pressure ($1\sim 6$ kg/cm²).

The following results were obtained:

1) d/a , d_0 , u_B , σ , ϵ of bubbles were determined over a range of $p_t=1\sim 6$ kg/cm², $G_p=0\sim 4$ cm³/sec. When data were correlated by G_p , approximately the same results as in the previous paper were obtained.

2) The values of E were calculated over a range of $p_t=1\sim 6$ kg/cm², $G_p=0\sim 0.54$ cm³/sec., $L=0.31\sim 0.51$, $1.2\sim 1.4$ cm³/sec. by diffusion model. E was affected greatly by G_p but scarcely by p_t and L . Data were correlated simply by $E \propto \exp(G_p)$.

Time Optimum Control for a Reactor with Two Types of Internal Feedback

Yuichi OGAWA

Abstract

A control which bring a reactor system to an equilibrium state in time optimum way is discussed. Non-linear integral equations containing the effects of two types of internal feedback and delayed neutrons and an external control system were adopted for the dynamic equations of the system. These equations were reduced to quasilinear (parametric) differential equations which were affected by the external control in the form of a combination of the control reactivity, its variational speed and the acceleration.

Pontryagin's Maximum Principle was applied to the quasilinear system and

several modes of optimum control patterns (nodal, focal, saddle and mixed) were obtained according to the nuclear and thermal properties, the thermal out-put of the reactor and the magnitude of the external control. Optimum control was obtained as the piecewise constant control with respect to the new control parameter which consists of a linear combination of the control reactivity, its speed and acceleration.

Measurement of the Corrosion Rate of Aluminium in NaCl Solution by the pH-static Method

Takashi MOROZUMI

Abstract

The corrosion rate of aluminium was determined in a H₂-saturated sodium chloride solution at 70°C by using the pH-static method. In contrast to the case of pure iron which was described in the previous report, a calibration for the hydrolysis of dissolved aluminium was required in accordance with the pH of solution for an estimation of the corrosion rate from the pH-stat current. The corrected rate of corrosion in 0.5N NaCl is given by the following equations,

$$\begin{aligned}\log i_{\text{corr}} &= 2.00 - 0.74\text{pH} && \text{at pH lower than 5,} \\ \log i_{\text{corr}} &= -9.38 + \text{pH} && \text{at pH higher than 8.}\end{aligned}$$

and in saturated NaCl solution,

$$\begin{aligned}\log i_{\text{corr}} &= 2.98 - \text{pH} && \text{at pH lower than 5,} \\ \log i_{\text{corr}} &= -9.70 + \text{pH} && \text{at pH higher than 8,}\end{aligned}$$

where i_{corr} is the corrosion rate given in mA/cm².

From the results of hydrolysis measurement, the predominant species of dissolved aluminium were postulated to be Al³⁺ in acidic, Al(OH)₃ in neutral and Al(OH)₄⁻ in alkaline solutions respectively.

An Electrochemical pCl-stat and Its Application to Electrometric Determination of Chloride Ion

Hiroshi OHASHI and Takashi MOROZUMI

Abstract

An electrochemical pCl-stat was devised with a silver-silver chloride electrode and a potentiostat to control the concentration of chloride ion in an aqueous solution

in a range of pCl 1 to 6.

Firstly, several attempts were made to construct a very stable potentiostat in which the fluctuation of potential was less than $\pm 10 \mu\text{V}$. Among the three types of electronic potentiostats examined, the most satisfactory one was constructed with a chopper-type differential amplifier.

Reasonably high accuracy of the pCl-stat in controlling the concentration of chloride ion was ascertained from the results of chemical analysis of chloride ion as a function of the potential of silver-silver chloride electrode and also the measurement of dynamic response of the pCl-stat.

It was also found that the pCl-stat can be successfully used for the electrometric determination of chloride ion in various cases, as follows :

- (1) the determination of free chloride ion in the presence of simple cations which do not form complex ions with chloride ion,
- (2) the determination of chloro-complex ion such as UO_2Cl^+ which can be formed by dissolving pure uranyl salt into a solution containing chloride ion, and
- (3) the determination of impurity chloride ion in the soluble salts which may form the chloro-complex.